Infrared emissivities of Mn, Co co-doped ZnO powders

Yao Yin-Hua(姚银华)† and Cao Quan-Xi(曹全喜)

School of Technical Physics, Xidian University, Xi'an 710071, *China*

(Received 25 February 2012; revised manuscript received 31 May 2012)

Infrared emissivities of $Zn_{0.99-x}Mn_{0.01}Co_xO$ (x = 0.00, 0.01, 0.03, 0.05) powders synthesized at different calcination temperatures by solid-state reaction are investigated. Their phases, morphologies, UV absorption spectra, and infrared emissivities are studied by XRD, SEM, UV spectrophotometer, and an IR-2 dual-band infrared emissometer in a range of 8 μm–14 μm. Doped ZnO still has a wurtzite structure, and no peaks of other phases originating from impurities are detected. The optical band-gap decreases as the Co content and calcination temperature ascend, and of which the smallest optical band gap is 2.19 eV. The lowest infrared emissivity, 0.754, is observed in $Zn_{0.98}Mn_{0.01}Co_{0.01}O$ with the increase in Co concentration. The infrared emissivity experiences fluctuations as the calcination temperature increases, and its minimum value is 0.762 at 1100 °C.

Keywords: co-doped ZnO, optical band gap, infrared emissivity, solid-state reaction

PACS: 42.79.Wc, 52.25.Tx, 71.55.Gs **DOI:** 10.1088/1674-1056/21/12/124205

1. Introduction

As an infrared stealth coating, doped semiconductor pigment can exhibit a low infrared emissivity (IR-e) by modifying some parameters properly, such as carrier concentration and carrier mobility. Up to now, ample research has been conducted regarding ITO (Sn-doped In_2O_3)[1,2] and ZAO (Al-doped ZnO).[3–5] Compared with ITO, ZnO has many advantages of low cost, non-toxicity, and simple preparation technique. Besides the electronic, piezoelectric, and optical applications,[6] doped ZnO can also be used as a low IR-e material. There are many studies concerning the effects of various preparation techniques on the IR-e. Zhu *et al.*[3] reported on the IR-e of ZAO films fabricated by sol–gel process. Wu *et al.*[4] and Wang *et al.*[5] studied the IR-e of ZAO films synthesized by liquid coprecipitation method and DC reactive magnetron sputtering, respectively. However, among a great deal of research work relating to the diluted magnetic semiconductors (DMSs),[7–11] very few studies on the IR-e of transition metal (TM) doped ZnO have been conducted. The resonant absorption, $\mathrm{Im}\,\varepsilon(\omega)$, can be modified by the susceptibility from the equation,[12]

$$\varepsilon(\omega)/\varepsilon_0 = 1 + \chi_{\mathrm{e}}, \tag{1}$$

where $\varepsilon(\omega)$, ε_0, and χ_{e} represent the dielectric function, vacuum dielectric function, and susceptibility, respectively. Based on Kirchoff's law, the IR-e will also be affected by the susceptibility indirectly.

In this study, $Zn_{0.99-x}Mn_{0.01}Co_xO$ (x = 0.00, 0.01, 0.03, 0.05) powders are prepared by standard solid-state reaction at different calcination temperatures. Their phases, morphologies, and IR-e values in a range of 8 μm–14 μm are investigated. The IR-e of ZnO powders is reduced by the incorporation of Co and Mn ions.

2. Experiment

According to certain proportions, ZnO was mixed with $MnCO_3$ and Co_2O_3. With alcohol as the solvent, the mixtures were ball milled in planetary mill (QM-1SP04). Then the mixtures were dried, grinded, and riddled with sifters. Finally, the mixed powders were calcined for 2 h in furnaces (sx2-6-13 box-type resistance furnace, Shanghai Laboratory Electric Furnace Works) and cooled in air. Besides pure ZnO at 1150 °C, $Zn_{0.99-x}Mn_{0.01}Co_xO$ (x = 0.00, 0.01, 0.03, 0.05) powders were prepared at 1000 °C, 1050 °C, 1100 °C, 1150 °C, and 1200 °C.

The structures of the samples were examined by using an X-ray diffractrometer (DX-1000, Dandong Fangyuan Co., Ltd.) with CuKα radiation at 35 kV and 25 mA. The grain sizes and morphologies of the samples were investigated by using a scanning electron microscope (SEM) (JSM 6360LV, JEOL). The UV spectra of samples were analysed by using a spectrophotometer (V-570, JASCO). The infrared emissivity was measured by an infrared emissometer (IR-

†Corresponding author. E-mail: yaoyinhua2009@126.com

© 2012 Chinese Physical Society and IOP Publishing Ltd

2 Dual-Band Emissometer, Shanghai Chengbo Optoelectronic Technology Co., Ltd.).

3. Results and discussion

From the pictures in Fig. 1, pure ZnO powders are white with a slightly yellow colour, while Mn, Co co-doped ZnO powders are green in colour, which becomes darker with Co concentration increasing.

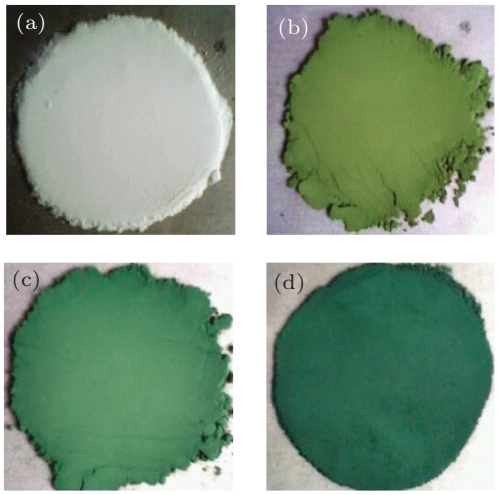


Fig. 1. (color online) Pictures of (a) pure ZnO and (b)–(d) $Zn_{0.99-x}Mn_{0.01}Co_xO$ (x = 0.01, 0.03, 0.05) powders synthesized at 1150 °C.

3.1. XRD analysis

By using software (MDI Jade 6), the co-doped samples are found to be still of wurtzite structure with no impurity phases from the magnified XRD patterns appearing in Fig. 2. It can be deemed that Mn and Co atoms have occupied the lattice sites of Zn atoms in zinc oxide, or exist as interstitial ions or atoms. However, we cannot exclude the existence of Mn and Co clusters and their oxide clusters whose amounts are too small to be detected in XRD.

The lattice parameters (a, c) are shown in Fig. 3, which are larger than those reported by Maensiri *et al.*[11] With a radius (0.080 nm) bigger than that of Zn^{2+} ion (0.074 nm),[13] Mn^{2+} ions occupy the sites of Zn^{2+} ions and cause an expansion in the lattice parameter of $Zn_{0.99}Mn_{0.01}O$ powders (x = 0.00). The same results are observed in Refs. [14]–[16], and it is deemed that Mn ions have replaced Zn ions. Through detailed XPS and XAFS analysis, Sun *et al.*[17] demonstrated that although MnO_2 was implanted into ZnO with a Mn^{4+} state, Mn atoms would substitute for Zn atoms with a Mn^{2+} state. Additionally, they mentioned many studies in which the same results were obtained. These are consistent with the XRD analysis in our work.

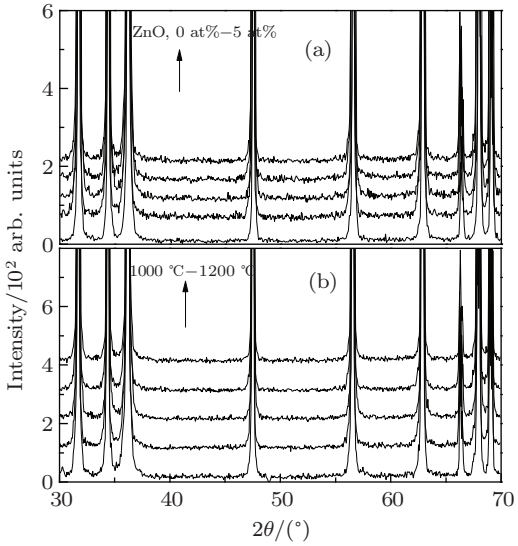


Fig. 2. XRD patterns of (a) $Zn_{0.99-x}Mn_{0.01}Co_xO$ (x = 0.00–0.05) at 1150 °C and (b) $Zn_{0.94}Mn_{0.01}Co_{0.05}O$ at different temperatures.

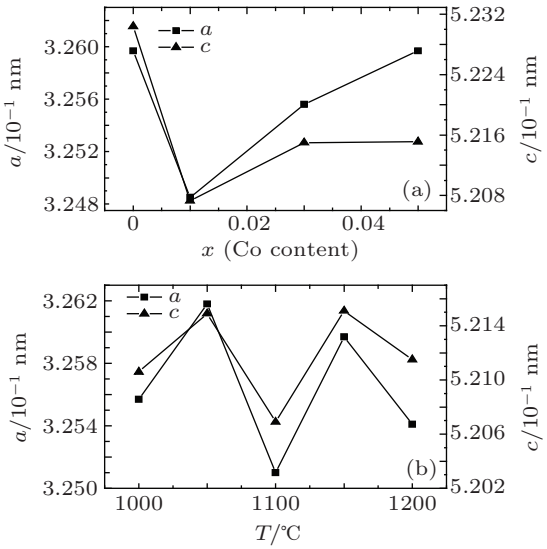


Fig. 3. Lattice parameters of (a) $Zn_{0.99-x}Mn_{0.01}Co_xO$ (x = 0.00–0.05) at 1150 °C and (b) $Zn_{0.94}Mn_{0.01}Co_{0.05}O$ at different temperatures.

The lattice parameter increases with the x value increasing from 0.01 to 0.05. From the radii of Co^{2+}, Co^{3+}, and Zn^{2+} ions (0.072 nm, 0.063 nm, and 0.074 nm, respectively),[13] the lattice parameter will be reduced by the replacement of Zn^{2+} by Co^{2+} or Co^{3+}. Therefore, it is not the substitutional doping that leads to the growing parameters but the formation of interstitial defects about Co or Zn.[18] From Fig. 3(b), the lattice parameters (a, c) experience the same fluctuations with calcination temperature increasing. At 1100 °C, the lattice parameter declines to a minimum value, smaller than those of

pure ZnO powders ($a = 0.32524$ nm, $c = 0.52071$ nm) calcined at 1100 °C. This implies that more Zn ions have been occupied by Co ions at this temperature.

3.2. SEM analysis

From the SEM images in Fig. 4(i), poor crystalline quality is seen clearly in pure ZnO powders. As expected, the introduction of Mn and Co ions improves the crystalline quality. The grain sizes decrease with Co content growing, which are 3.77 μm, 3.26 μm, and 2.66 μm, respectively. As the calcination temperature rises, the grain sizes are 1.81 μm, 1.79 μm, 2.07 μm, 2.66 μm, and 4.37 μm, respectively. Clear grain surfaces can be observed in $Zn_{0.98}Mn_{0.01}Co_{0.01}O$ powders prepared at 1150 °C. However, the particles show slight aggregations in the samples calcined at higher temperatures.

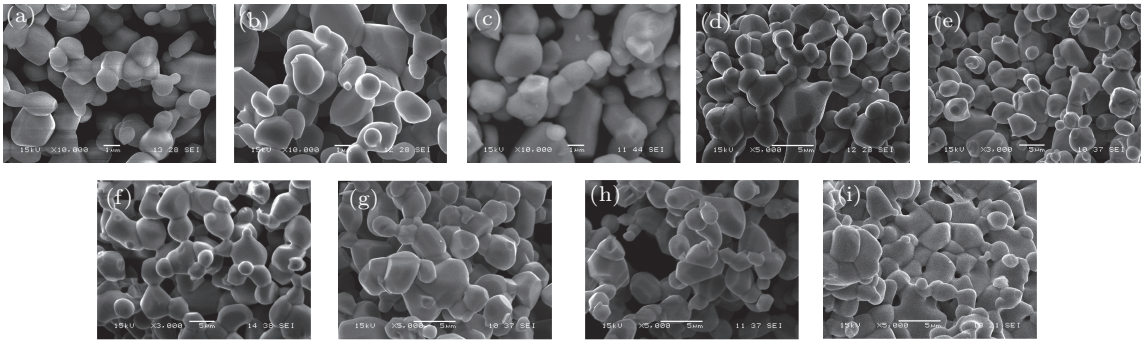


Fig. 4. SEM images of (a)–(e) $Zn_{0.94}Mn_{0.01}Co_{0.05}O$ at 1000 °C–1200 °C, (f)–(h) samples with 0 at%–3 at% Co, and (i) pure ZnO powders.

3.3. UV absorption spectrum analysis

Figure 5 shows the UV absorption spectra of samples. The optical absorptions, α, between 500 nm and 700 nm are enhanced with Co content and calcination temperature increasing. A red shift of absorption edge can be seen in the samples doped by Mn and Co ions.

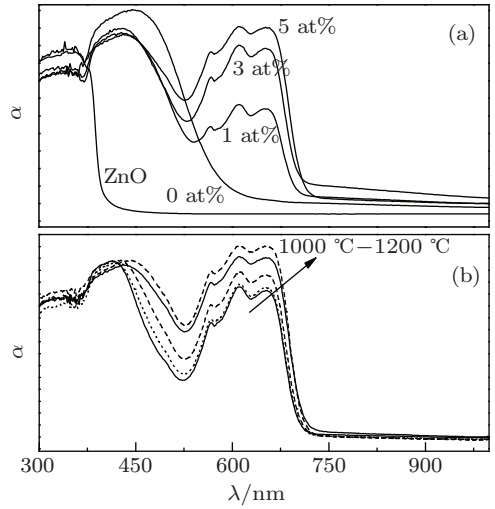


Fig. 5. UV absorption spectra of (a) $Zn_{0.99-x}Mn_{0.01}Co_xO$ at 1150 °C and (b) $Zn_{0.94}Mn_{0.01}Co_{0.05}O$ at different temperatures.

The optical band gap, E_g, can be estimated by the following equation:[19]

$$(\alpha h\nu)^2 = A(h\nu - E_g), \tag{2}$$

where A is constant, h represents Planck's constant, and ν is the frequency of the electromagnetic wave. The dependence of $(\alpha h\nu)^2$ on $h\nu$ is displayed in Fig. 6. Figure 6(a) shows that the values of E_g decrease with Co concentration increasing from 1 at% to 5 at%, which are 2.34 eV, 2.28 eV, and 2.19 eV, respectively. In addition, a decreasing optical band gap (2.25 eV) is also detected in $Zn_{0.99}Mn_{0.01}O$ powders ($x = 0.00$). Although these values are much smaller than those in Refs. [20] and [21], the same relationships

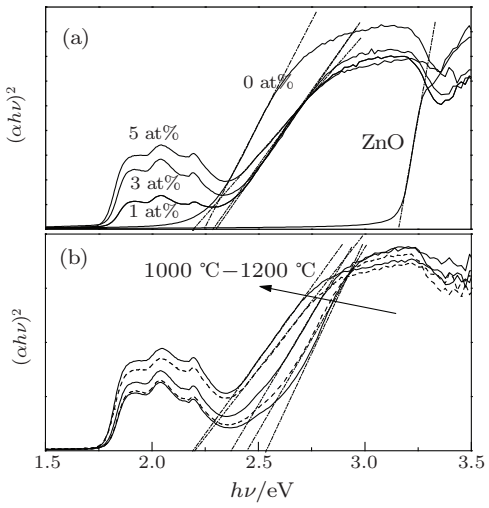


Fig. 6. Dependences of $(\alpha h\nu)^2$ on $h\nu$ in samples (a) with different Co contents and (b) at different temperatures.

between band gap and Co content are found. Ullah and Dutta[22] and Polyakov *et al.*[23] also observed the declining optical band gaps in Mn- and Co-doped ZnO. However, Ozerov *et al.*[24] reported on a contrary result. Figure 6(b) indicates that when the temperature is elevated, the values of E_g decrease in $Zn_{0.94}Mn_{0.01}Co_{0.05}O$, which are 2.54 eV, 2.44 eV, 2.34 eV, 2.20 eV, and 2.19 eV, respectively. Maensiri *et al.*[11] obtained the same conclusion, but a bigger optical band gap, about 3.2 eV, was detected in their studies. The band structural change is attributed to the replacement of Zn ions by Mn and Co ions.[11]

3.4. Infrared emissivity analysis

3.4.1. Effect of Co concentration

The IR-e values of samples, dependent on x values and calcination temperatures, are presented in Fig. 7. Pure ZnO powders calcined at 1150 °C show a high IR-e value, 0.812. After being implanted into ZnO, both Mn and Co ions can lower the IR-e value. From Fig. 7(a) it follows that the IR-e value shows the same relationship as that between lattice parameter and Co concentration. Co_2O_3 starts to resolve into CoO at high temperatures via the following reaction:[25]

$$2Co_2O_3 \xrightarrow{1000\ ^\circ C} 4CoO + O_2 \uparrow. \quad (3)$$

Having an ion radius (0.072 nm) similar to that of Zn^{2+} (0.074 nm), Co^{2+} ions can occupy the sites of Zn^{2+} ions easily. Moreover, CoO possesses Co vacancy defects and ZnO has oxygen vacancy defects.[13] Consequently, replacing the sites of Zn^{2+} ions, the produced Co^{2+} ions can reduce the boundary defects and lattice distortion. As a result of degraded carrier scattering and raised carrier mobility, the elevated conductivity contributes to the lower IR-e. Additionally, CoO also plays an important role in enhancing the carrier concentration. From the following reaction:[25]

$$CoO \longrightarrow Co_{Zn} + V_o^{2+} + \frac{1}{2}O_2 + 2\,e, \quad (4)$$

the introduction of CoO will raise the carrier concentration by increasing the oxygen vacancies.

This is different from ZAO in which Al ions provide an additional electron. As a result, the growing conductivity restrains the increase of the IR-e. When the Co content is 1 at%, the emissivity is lowest (0.754) due to the completive replacement of Zn ions by Mn and Co ions. However, as Co concentration grows, the formation of more interstitial defects about Co or Zn results in the lattice distortion. On the other hand, from the SEM analysis, the decreasing grain size brings about more grain boundaries. Then, the carrier scattering is enhanced, thereby depressing the carrier mobility and conductivity. In conclusion, the increasing of infrared emissivity arises from the minimized conductivity and poor crystalline quality.

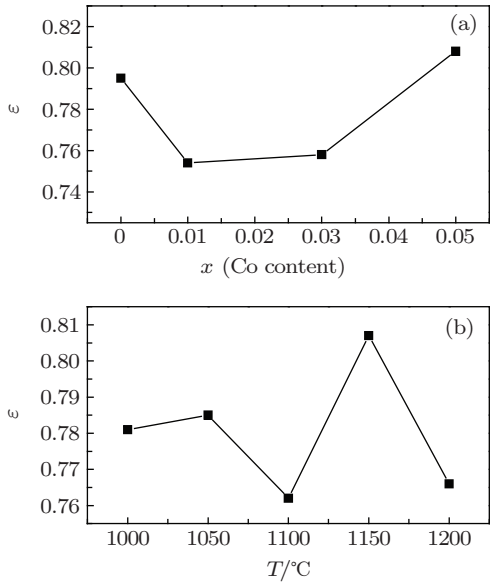


Fig. 7. IR-e values of (a) $Zn_{0.99-x}Mn_{0.01}Co_xO$ at 1150 °C and (b) $Zn_{0.94}Mn_{0.01}Co_{0.05}O$ at various temperatures.

3.4.2. Effect of calcination temperature

Just like the lattice parameter, the IR-e value experiences fluctuations with calcination temperature increasing (see Fig. 7(b)). When the lattice parameter declines, the IR-e value also goes down. However, in general, the IR-e value first ascends and then descends. As the calcination temperature jumps, the lower lattice parameters are attributed to the replacement of Zn ions by Co ions. As discussed above, the IR-e value can be reduced by the substitution of Co^{2+} ions for Zn^{2+} ions. Besides, further calcination is beneficial to the desorption of adsorbed oxygen on the grain boundary and fewer electron capturing traps.[3,7] As a consequence, the carrier concentration increases and the IR-e value descends. The lowest IR-e value (0.762) is obtained at 1100 °C. Nevertheless, a higher calcination temperature will lead to the secondary crystallization of the sample and abnormal enlargement of grains (see Fig. 4(d)). And the crystalline

quality of grain becomes poor. The lattice symmetry is destroyed and the infrared absorption is enhanced, which is followed by a higher IR-e value. Close to the IR-e value of pure ZnO (0.841), the highest IR-e value (0.808) is reached in $Zn_{0.94}Mn_{0.01}Co_{0.05}O$ powder at 1150 °C.

3.5. XPS spectra analysis

To study the chemical states of Mn and Co ions in $Zn_{0.94}Mn_{0.01}Co_{0.05}O$ powder synthesized at 1100 °C, XPS measurement is performed with an emphasis on the peaks associated with Mn2p and Co2p by using a multi-technique electron spectrometer (ESCALAB MK II, VG Scientific Ltd). TheMgKα radiation is used, and all binding energies are referenced to C 1s photoelectron signal at 285 eV.

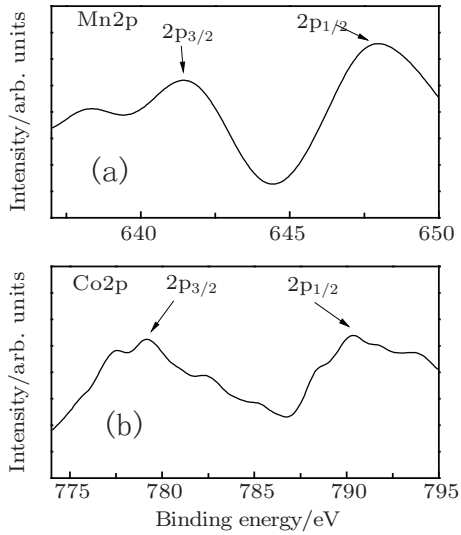


Fig. 8. XPS spectra of (a) Mn2p and (b) Co2p in $Zn_{0.94}Mn_{0.01}Co_{0.05}O$ calcined at 1100 °C.

It is clearly seen from the XPS spectra in Fig. 8(a) that $Mn2p_{3/2}$ peaks are located at 641 eV, showing that Mn ions in the powder are mainly in a chemical state of Mn^{2+}.[26] Mn clusters are not detected according to the difference between $Mn2p_{3/2}$ and $Mn2p_{1/2}$. This is in good agreement with the XRD analysis. The peak at 779.30 eV attributed to $Co2p_{3/2}$ (Co^{2+} multiple sp;itting) is shown in Fig. 8(b).[26] And from the difference between $Co2p_{3/2}$ and $Co2p_{1/2}$, no Co cluster but Co^{2+} ions exist in the sample. The same results can be found in Refs. [9] and [10]. However, the valence of Co is not easily determined by XPS. Because the number of Co^{3+} ions can be too small to be detected, the existence of Co^{3+} ions is not excluded. The result indicates that the emissivity can be lessened by the substitution of Co^{2+} ions for Zn ions.

4. Conclusion

$Zn_{0.99-x}Mn_{0.01}Co_xO$ (x = 0.00, 0.01, 0.03, 0.05) powders were synthesized at various calcination temperatures by solid-state reaction. No secondary phase was detected in each of the fabricated samples. This demonstrates that Co and Mn atoms can enter into the ZnO lattice easily. The higher the Co content and the calcination temperature, the smaller the optical band gap is. The observed optical band gaps are much smaller than those obtained by other authors. For each of the samples, the emissivity and the lattice parameter vary with Co content and calcination temperature in the same manner. The lowest infrared emissivity (0.754) is obtained in $Zn_{0.98}Mn_{0.01}Co_{0.01}O$ prepared powder at 1150 °C. XPS spectra imply that Mn and Co ions are dissolved in the ZnO lattice with Mn^{2+} and Co^{2+}, respectively.

References

[1] Chao Y P, Tang W, Weng X L and Deng L J 2011 *Mater. Sci. Forum* **687** 771

[2] Biswas P, De A, Pramanik N, Chakraborty P, Ortner K, Hock V and Korder S 2003 *Mater. Lett.* **57** 2326

[3] Zhu D M, Li K, Luo F and Zhou W C 2009 *Appl. Surf. Sci.* **255** 6145

[4] Wu X W, Feng Y J and Liu Y K 2010 *J. Harbin Inst. Technol.* (New Series) **17** 588

[5] Wang W W, Diao X G, Wang Z, Wang T M 2005 *Journal of Beijing University of Aeronautics and Astronautics* **31** 236 (in Chinese)

[6] Chowdhury R, Adhikari S and Rees P 2010 *Physica* B: *Condens. Matter* **405** 1

[7] Lin M N, Hsu H S, Lai J Y, Guo M C, Lin C Y, Li G Y, Chen F Y, Huang J J, Chen S F, Liu C P and Huang J C A 2011 *Appl. Phys. Lett.* **98** 212509

[8] Pearton S J, Norton D P, Ivill M P, Hebard A F, Zavada J M, Chen W M and Buyanova I A 2007 *J. Electron. Mater.* **36** 462

[9] Cong C J, Hong J H and Zhang K L 2009 *Mater. Chem. Phys.* **113** 438

[10] Wang L W, Xu Z, Zhang F J, Zhao S L and Lu L F 2010 *Int. J. Miner. Metall. Mater.* **17** 476

[11] Maensiri S, Laokul P, Klinkaewnarong J and Thomas C 2009 *Appl. Phys.* A **94** 602

[12] Jackson J D 1999 *Classical Electrodynamics* 3rd edn. (New York: Wiley) pp. 310–312

[13] Zhou Y 2004 *Ceramic Materials* 2nd edn. (Beijing: Science Press) p. 12 (in Chinese)

[14] Doria J, Mera J, Córdoba C, Paredes O, Gomez A, Paucar C and Moran O 2011 *Revista Colombiana de Física* **43** 824

[15] Maiti U N, Ghosh P K, Nandy S and Chattopadhyay K K 2007 *Physica* B: *Condens. Matter* **387** 104

[16] Abrishami M E, Hosseini S M and Kompany A 2011 *J. Appl. Sci.* **11** 1411

[17] Sun B, Zhao C Y, Xu P S, Zhang G B and Wei S Q 2007 *J. Inorg. Mater.* **22** 912

[18] Yu Y S, Kim G Y, Min B H and Kim S C 2004 *J. Eur. Ceram. Soc.* **24** 1866

[19] Peng L P, Fang L and Wu W D 2012 *Chin. Phys.* B **21** 047305

[20] Sarsari I A, Salamati H, Kameli P and Razavi F S 2011 *J. Supercond. Nov. Magn.* **24** 2294

[21] Ramachandran S, Tiwari A and Narayan J 2004 *J. Electron. Mater.* **33** 1301

[22] Ullah R and Dutta J 2008 *J. Hazard. Mater.* **156** 196

[23] Polyakov A Y, Smirnov N B, Govorkov A V, Kozhukhova E A, Heo Y W, Ivill M P, Ip K, Norton D P, Pearton S J, Kelly J, Rairigh R, Hebard A F and Steiner T 2005 *J. Vac. Sci. Technol.* B: *Microelectron. Nanometer Structure* **23** 276

[24] Ozerov I, Chabre F and Marin W 2005 *Mater. Sci. Eng.* C **25** 615

[25] Han W, Wang J W and Meng M 2005 *Insulators and Surge Arresters* **1** 33 (in Chinese)

[26] Wagner C D, Riggs W M, Davis L E, Moulder J F and Muilenberg G E 1979 *Handbook of X-ray Photoelectron Spectroscopy* (Eden Prairie: Perking-Elmer Corporation, Physical Electronics Division) p. 74